



Cite this: *Chem. Commun.*, 2019, 55, 13267

Received 9th September 2019,
Accepted 3rd October 2019

DOI: 10.1039/c9cc07009e

rsc.li/chemcomm

Monoamine oxidase-A targeting probe for prostate cancer imaging and inhibition of metastasis†

Won Young Kim,^{‡a} Miae Won,^{ib ‡a} Abbas Salimi,^{‡b} Amit Sharma,^{ib a} Jong Hyeon Lim,^c Seung-Hae Kwon,^d Joo-Yeong Jeon,^d Jin Yong Lee^{ib *c} and Jong Seung Kim^{ib *a}

Mitochondrial enzyme monoamine oxidase (MAO-A) is known to be overexpressed in prostate cancer (PCa) cells. Herein, we have developed a two-photon probe (PCP-1) for selectively targeting and imaging the MAO-A in PCa. Supported by enzymatic docking and *in vitro* experiments, PCP-1 showed efficiency to visualize MAO-A overexpressing cells and inhibit their growth and metastasis potential.

Prostate cancer (PCa), is the second leading cause of cancer-related deaths among most male patients in the world.¹ The incidence rate is high with all ages in America followed by Australia/New Zealand and Europe. Cancer metastasis, in general, primarily causes human cancer deaths to the extent of more than 90%.² PCa progresses slowly, and as a result many patients die because of competing causes. Thus, accurate detection of PCa and its metastatic potential is considered to be needed to decide the exact tumor stage in patients and the correct treatment plan in clinical practices.^{3,4} Widespread use of prostate specific antigen (PSA) level testing in patients has led to a drastic increase in diagnosis and therapy,⁶ but sometimes patients don't receive benefits from intervention due to either the indolent or disseminated state of the disease at the diagnosis stage. Moreover, this test exhibits low specificity because PSA levels are also elevated in patients with benign prostatic hyperplasia.⁵ This low specificity can lead to excessive treatments of early-stage and less aggressive cancers⁶ and it is both time and money consuming with poor clinical outcomes. Hence, the search for alternate targets and development of sensitive detection tools with high tumor-targeting specificity are urgently needed.

Recent studies have shown that increased levels of monoamine oxidase-A (MAO-A) are associated with PCa progression and inhibition of MAO-A activities prevents the growth of PCa cells *in vitro* and tumor xenografts *in vivo*.⁷ MAO-A is a mitochondria-bound enzyme which catalyzes the oxidative deamination of neurotransmitters and dietary amines.⁸ This process produces hydrogen peroxide (H₂O₂), a major source of reactive oxygen species (ROS), which can damage the DNA of cancer cells, the main cause of tumor initiation and progression.⁹ Moreover, previous studies strongly support that excessive intracellular levels of H₂O₂ produced by MAO-A are responsible for inducing the epithelial to mesenchymal transition (EMT) in PCa. MAO-A-mediated generation of ROS is also associated with activation of the transcription factor HIF-1 α (a master regulator of hypoxia)¹⁰ which further increases the level of ROS and ultimately drives PCa progression and metastasis.¹¹ In this work, MAO-A was identified as an important target for the selective detection of human PCa *in vitro*.

Recently, fluorescence imaging has become the most prominent tool in bio-imaging related studies.¹² Fluorescence-based diagnosis are fast, noninvasive, sensitive and selective tools for treatment estimation in oncology. Until near-infrared (NIR) fluorophores were used, otherwise, most of the reported fluorophores were associated with common shortcomings like poor tissue penetration of the excitation or emission lights when applied to mouse or animal models.¹³ Alternatively, we chose a reporter with two-photon (TP) excitation capability because it would be ideal for *in vitro* bio-imaging as well as *in vivo* real-time monitoring. Deep tissue penetration of TP fluorescence enhances the microscopic images and its weak excitation energy reduces undesired tissue damage.¹⁴ It may also facilitate the *in vivo* tumor imaging and differentiation of tumors from surrounding normal tissues and organs.

In view of the aspects mentioned above, in this investigation, a novel TP fluorescent probe **PCP-1** for targeting MAO-A was designed. This was achieved by conjugating a MAO-A selective inhibitor (moclobemide)¹⁵ with a TP fluorophore to improve excitation permeability for imaging. The **PCP-1** can selectively bound to MAO-A, overexpressed in the PCa (Scheme 1). Thus,

^a Department of Chemistry, Korea University, Seoul 02841, Korea.

E-mail: jongskim@korea.ac.kr

^b School of Chemical Engineering, Sungkyunkwan University, Suwon 16419, Korea

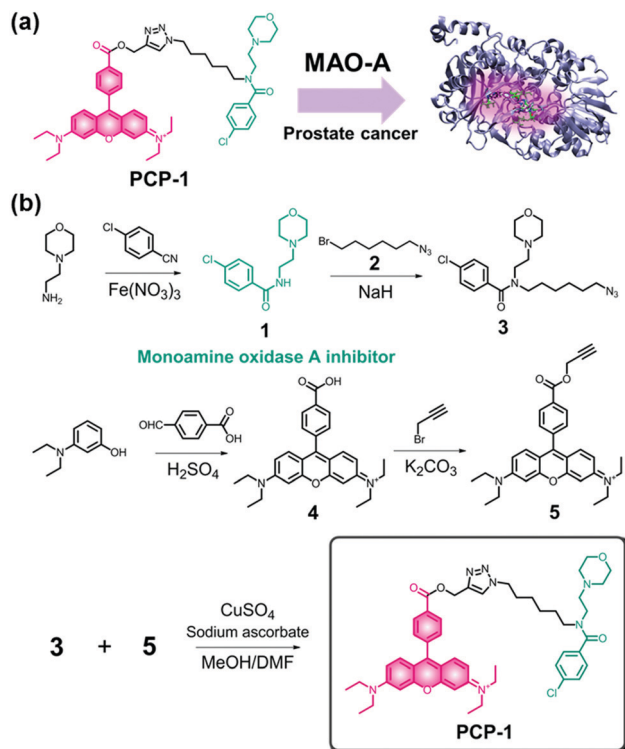
^c Department of Chemistry, Sungkyunkwan University, Suwon 16419, Korea.

E-mail: jinyilee@skku.edu

^d Seoul Center, Korea Basic Science Institute, Seoul 02841, Korea

† Electronic supplementary information (ESI) available. See DOI: 10.1039/c9cc07009e

‡ These authors contributed equally to this work.



Scheme 1 (a) Design of **PCP-1** targeting MAO-A for the detection of prostate cancer (PCa) and (b) synthetic scheme of **PCP-1**.

this probe may allow the prostate tumors to be optically discerned from normal tissues by *in vivo* TP fluorescence without surgical methods. In addition, it can prevent cancer cell proliferation and metastasis by inhibition of MAO-A activities.

The probe **PCP-1** was successfully synthesized and was analytically characterized by ^1H , ^{13}C NMR and MS (ESI †). The synthesis of probe **PCP-1** is shown in Scheme 1b. Briefly, a TP fluorophore, *i.e.*, rhodamine derivative with a terminal alkyne functionality (5), was conjugated with the MAO-A inhibitor carrying an azide group (3) by using the Cu(I)-mediated azide-alkyne cycloaddition reaction, generating a triazole moiety which is easy to synthesize and does not interfere with the biological environment *in vivo*.¹⁶ To minimize the steric influence of the fluorophore on the binding interaction between the synthetic inhibitor (moclobemide) and MAO-A enzyme, a six-carbon alkyl chain was selected as a linker between the fluorophore and the inhibitor.¹⁷

To initially confirm the interaction of the probe **PCP-1** towards MAO-A enzyme, a docking study and further molecular dynamics (MD) simulation (Fig. 1) were performed to understand the binding properties at the atomic level. After MD simulations, a binding free energy of $-118.6 \text{ kcal mol}^{-1}$ was obtained, and the residual interactions are shown in Fig. S9 (ESI †). The simulation data confirmed that the inhibitor was not sterically hindered by the linker and tagged fluorescent group, indicating that probe **PCP-1** was successfully designed for binding with MAO-A.

In order to verify the photochemical function of a TP fluorophore, density functional theory (DFT) calculations (Fig. S10 and S11, ESI †) were performed. The calculated TP absorption

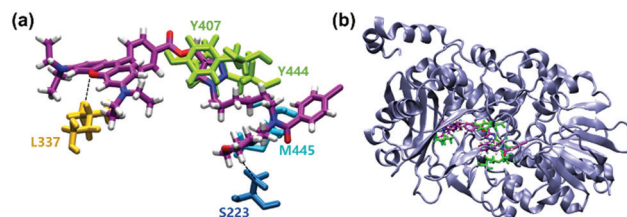


Fig. 1 (a) Residual interactions within binding sites of human MAO-A and probe **PCP-1** (pink). (b) Representative structure obtained from the docking study (PDB Code: 2Z5X).

wavelength of the TP fluorophore for first to third excited states were 920 nm, 808 nm and 792 nm with a two-photon cross-sections of 460 GM, 404 GM, and 396 GM (Goepfert-Mayer), respectively. The calculated data was substantiated by comparison to the reference dye, implying the selected TP fluorophore can promise ideal functions as a bio-imaging probe for PCA (Fig. S10, ESI †).

In order to test whether the probe **PCP-1** could be used as an imaging probe for PCa, the optical properties of probe **PCP-1** in aqueous environments were investigated. UV-Vis analysis of probe **PCP-1** (10 μM) in phosphate saline buffer (PBS) solution (pH 7.4, containing 0.2% DMSO v/v) showed an absorption maximum at 566 nm, characteristic of the rhodamine moiety (Fig. S12a, ESI †). Upon excitation at 566 nm, probe **PCP-1** exhibited a strong fluorescence emission band centered at 600 nm (Fig. 2a). Further, absorption and emission bands of probe **PCP-1** changed negligibly under both acidic and alkaline environments (pH 3–10) (Fig. S12 and S2b, ESI †). This result suggests that probe **PCP-1** is unlikely to be affected by the acidic pH environments of a tumor.

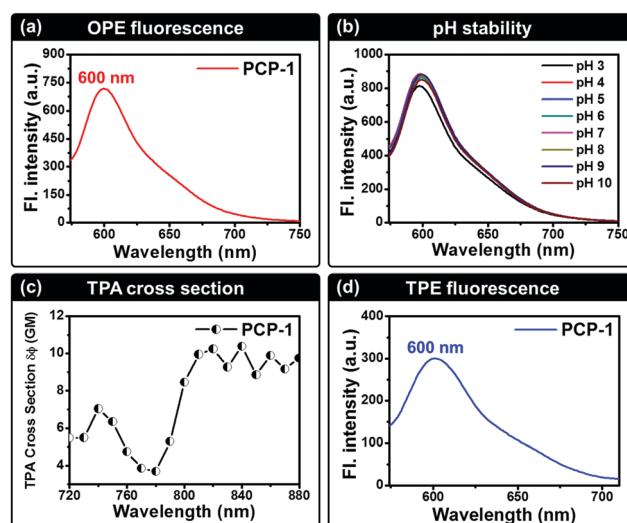


Fig. 2 (a) Fluorescence spectra of MAO-A-targeted two-photon probe **PCP-1** (10 μM) in 10 mM PBS buffer (pH 7.4, 0.2% DMSO, 37 $^\circ\text{C}$), $\lambda_{\text{ex}} = 566 \text{ nm}$, $\lambda_{\text{em}} = 600 \text{ nm}$. (b) Fluorescence intensity change with varying pH range of the solutions (DMSO-water, 0.2% v/v), $\lambda_{\text{ex}} = 566 \text{ nm}$, $\lambda_{\text{em}} = 600 \text{ nm}$. (c) Two-photon action cross section spectra of **PCP-1** (10 μM) in PBS buffer (37 $^\circ\text{C}$). (d) Two-photon fluorescence spectra of **PCP-1** in 10 mM PBS buffer (pH 7.4, 0.2% DMSO, v/v), $\lambda_{\text{ex}} = 830 \text{ nm}$, $\lambda_{\text{em}} = 600 \text{ nm}$.

Next, to explore the TP imaging ability of probe **PCP-1** under physiological conditions, TP excitation spectra of **PCP-1** (10 μ M) was investigated in a PBS buffer. As shown in Fig. 2c, the GM values (δ_{ϕ}) of probe **PCP-1** over absorbance $\lambda_{\text{abs}} = 810$ nm reached a maximum, corresponding to results from the calculated TP absorption data above. Subsequently, **PCP-1** was irradiated at 830 nm in PBS solutions (pH 7.4, 0.2% DMSO v/v). As expected, a fluorescence emission band was observed centered at 600 nm upon irradiation (Fig. 2d). These experiments successfully demonstrated the potential of probe **PCP-1** for TP imaging of PCa as it was sufficiently stable in physiological conditions, able to produce a strong fluorescent emission and has two-photon properties. These features are inevitably required for small-molecule imaging in the cells.

Following the encouraging results described above, various *in vitro* cell tests were performed. First, in order to examine the targeting ability of **PCP-1** for PCa, TP images were confirmed in various cell lines with different MAO-A expression levels. Before that, an immunoblot assay was performed to compare the MAO-A expression levels in four human cancer cell lines, namely, LNCap (prostate cancer), MDA-MB-231 (breast cancer), HepG2 (liver cancer), and A549 (lung cancer) cells, respectively. Among these four tested cell lines, LNCap cells exhibited the highest levels of MAO-A enzyme (Fig. S13, ESI[†]). Subsequently, the probe **PCP-1** (10 μ M) was treated with each cell line using incubation for 24 h. As expected, **PCP-1** emitted the highest fluorescence intensity with the LNCap cell line, exhibiting a noticeable difference among the other tested cell lines, which is in accordance with the MAO-A expression levels in these cells (Fig. 3a). An excellent cell permeability of **PCP-1** was also confirmed.

Next, to examine the retention ability of **PCP-1**, time-dependent fluorescence imaging was performed in the cell lines. As shown in Fig. 3b, the probe **PCP-1** showed significant fluorescence emission in the LNCap cell line with sufficient time (48 h), which is the required characteristic for successful *in vivo* imaging. In addition, to validate whether the probe **PCP-1** binds with MAO-A in the cancer cells, inhibition studies were conducted. Clorgyline, a selective inhibitor of MAO-A enzyme, was pretreated (100 μ M) in LNCap cells prior to incubation with **PCP-1**. The results showed a noticeable reduction in fluorescence intensity in the LNCap cell (Fig. S14 and S15, ESI[†]). These results support that a strong fluorescence and increased retention in the PCa cell are caused by the MAO-A targeting unit of **PCP-1** which selectively binds with MAO-A.

Moreover, the colocalization of probe **PCP-1** was also examined by confocal microscopy upon co-incubation with the commercial Mito (mitochondrial), Lyso (lysosomal) and ER (endoplasmic reticulum) trackers. As shown in confocal merged images (Fig. 3c), the fluorescence of **PCP-1** was completely localized with the Mito tracker. Since the MAO-A enzyme is bound to the outer membrane of mitochondria in a cell, **PCP-1**'s localization in the mitochondria is the inevitable result. Subsequently, changes in the membrane potentials of mitochondria in each of the cell lines were determined by a membrane potential (MMP) assay. Clearly, the LNCap cell exhibited the lowest mitochondria membrane potential (Fig. 3d) upon treatment with **PCP-1**. These results demonstrated that the reason for **PCP-1** accumulation in cancer cell mitochondria is not

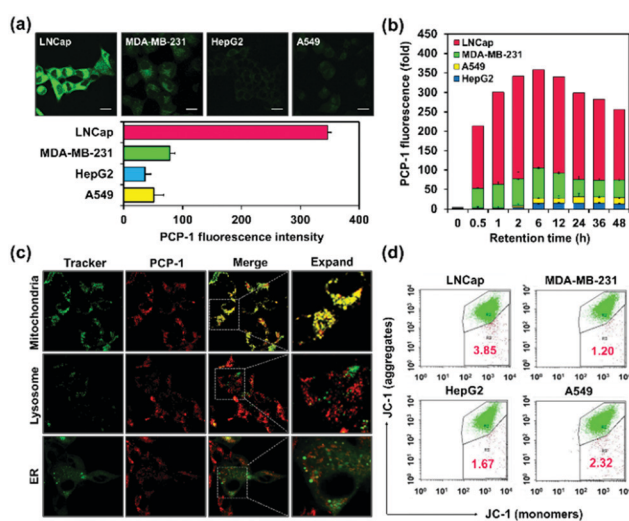


Fig. 3 (a) TP cell images of human cancer cells; LNCap (prostate adenocarcinoma), MDA-MB-231 (breast adenocarcinoma), HepG2 (hepatocellular carcinoma), and A549 (lung adenocarcinoma) cells treated with **PCP-1**. The cells were incubated with HBSS containing the probe (10 μ M) and then the images were obtained. $\lambda_{\text{ex}} = 830$ nm; $\lambda_{\text{em}} = 500\text{--}700$ nm. (b) Retention time assay for fluorescence intensity changes of **PCP-1** in various tested cancer cells. (c) Colocalization images of **PCP-1** and sub-organelles (Mitochondria, Lysosome, and ER). (d) Mitochondria membrane potential measurement in various cancer cells upon treatment with **PCP-1**.

due to the fluorophore, but rather to the targeting effect of the MAO-A inhibitor used in **PCP-1**. Together, these experimental results indicated that the probe **PCP-1** has excellent MAO-A target ability and can selectively detect PCa as a promising bio-imaging probe.

Recent reports suggested that overexpression of MAO-A in human PCa cells enhances cancer cell growth and induces EMT.¹⁰ Therefore, we examined cell viability and migration assays to test the ability of **PCP-1** to inhibit MAO-A activity in PCa cells. LNCap cells were treated with rhodamine fluorophore, moclobemide and clorgyline as control groups and **PCP-1**, respectively. As shown in Fig. 4a and Fig. S16a (ESI[†]), the group treated with **PCP-1** exhibited a remarkable reduction in cell viability in a dose-dependent manner, while cells treated the fluorophore (rhodamine) showed only a little effect even at high doses. This result showed that PCa cell growth was suppressed by the MAO-A inhibitor of **PCP-1** impeding the MAO-A activity. Compared with **PCP-1**, the groups treated with clorgyline and moclobemide, respectively also showed a decrease in cell viability but less than **PCP-1** (Fig. 4b and Fig. S16b, ESI[†]). Thus, **PCP-1** has a better targeting and inhibition effect on MAO-A's activities, which may have resulted from the preferential mitochondria targeting effect of **PCP-1**. The effective cell death mechanism of **PCP-1** was also investigated by Western blot and Annexin V/PI (Fig. 4c and d). The reduced expression of the MAO-A protein by **PCP-1** in LNCap cells induced cell death, which was demonstrated by increased BAX (pro-apoptotic protein) and decreased BCL-2 (anti-apoptotic protein) expressions. Also, the level of cleaved caspase 3 was enhanced by **PCP-1** treatment (Fig. 4c). Further, the Annexin-V/PI staining assay confirmed that **PCP-1** treatment increased the Annexin

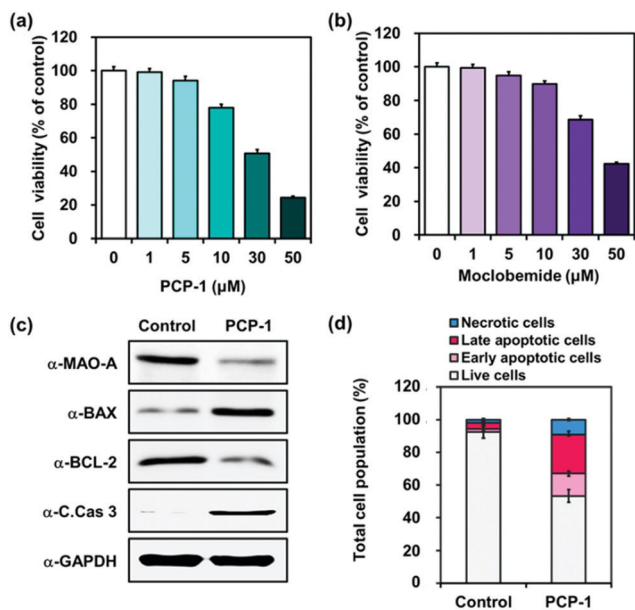


Fig. 4 PCP-1 induced cell death. Cell viability of PCP-1, and moclobemide. Cells were incubated with 0, 1, 5, 10, 30 and 50 μM of PCP-1 (a), and moclobemide (b) for 24 h in LNCap cells. Values represent mean \pm SE of three independent experiments performed in triplicate; * $p < 0.05$. (c) Cell death-related protein expression levels by PCP-1 in LNCap cells are shown by Western blot assay. (d) AnnexinV/PI staining assay in LNCap cells incubated with the PCP-1 (10 μM) and then the values were obtained for 24 h (control group treated with 1% DMSO).

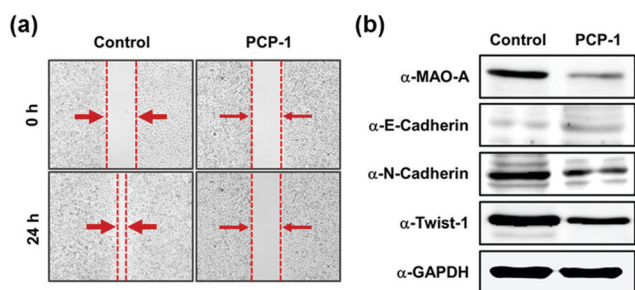


Fig. 5 PCP-1 inhibits EMT related to metastasis in prostate cancer cells. (a) Cell migration assay in LNCap cells incubated with the PCP-1 (10 μM) and then the images were obtained for 24 h (control group treated with 1% DMSO). (b) The expression of EMT-related markers, *E*-cadherin, *N*-cadherin, and Twist-1 was observed after PCP-1 (10 μM) treatment using Western blot assay.

V-positive apoptotic cells population (by 40%) compared to the control (Fig. 4d).

To investigate the metastatic potential inhibition of LNCap cells by PCP-1, we used a cell migration assay. After treatment with PCP-1 (10 μM , 48 h) in LNCap cell lines, a significant reduction in migration of PCP-1 treated cells were observed as compared to the control group (Fig. 5a). Further, *E*-cadherin was upregulated whereas *N*-cadherin and Twist-1 were significantly downregulated in LNCap cells treated with PCP-1, suggesting that PCP-1 could inhibit EMT in PCa (Fig. 5b). These

results were attributed to PCP-1's ability to inhibit MAO-A's activity, thereby suppressing prostate cancer cell growth, proliferation and preventing their metastatic potential.

In conclusion, a new TP imaging probe (PCP-1) was developed. PCP-1 was preferentially taken up and retained in the MAO-A overexpressing PCa cells (LNCap) over other tested human cancer cell lines. Furthermore, the remarkable selectivity towards MAO-A was also supported by enzymatic docking studies. In addition, PCP-1 showed a significant inhibition effect on PCa cell growth, proliferation, and cancer metastasis by inhibiting MAO-A's activities. These results, therefore, suggest that the probe PCP-1 will be highly applicable for further *in vivo* imaging and the design of targeted therapeutics for PCa in the future.

This work was supported by the National Research Foundation of Korea (NRF) funded by the Ministry of Science and ICT (CRI project no. 2018R1A3B1052702 and NRF-2019M3E5D1A01068998, J. S. K.), and the Basic Science Research Program (2017R1D1A1-B03030062, M. W.) funded by the Ministry of Education. This work was also supported in part by Korea Basic Science Institute Grant (T38662).

Conflicts of interest

There are no conflicts to declare.

Notes and references

- R. L. Siegel, K. D. Miller and A. Jemal, *Ca-Cancer J. Clin.*, 2016, **66**, 7–30.
- C. L. Chaffer and R. A. Weinberg, *Science*, 2011, **331**, 1559–1564.
- T. Aikou, Y. Kitagawa, M. Kitajima, Y. Uenosono, A. J. Bilchik, S. R. Martinez and S. Saha, *Cancer Metastasis Rev.*, 2006, **25**, 269–277.
- R. Siegel, E. Ward, O. Brawley and A. Jemal, *Ca-Cancer J. Clin.*, 2011, **61**, 212–236.
- L. D. Papsidero, M. C. Wang, L. A. Valenzuela, G. P. Murphy and T. M. Chu, *Cancer Res.*, 1980, **40**, 2428–2432.
- D. Bates, S. Abraham, M. Campbell, I. Zehbe and L. Curiel, *PLoS One*, 2014, **9**, e97220.
- V. Flamand, H. J. Zhao and D. M. Peehl, *J. Cancer Res. Clin. Oncol.*, 2010, **136**, 1761–1771.
- M. Bortolato, K. Chen and J. C. Shih, *Adv. Drug Delivery Rev.*, 2008, **60**, 1527–1533.
- S. Josson, T. Nomura, J. T. Lin, W. C. Huang, D. Q. Wu, H. E. Zhou, M. Zayzafoon, M. N. Weizmann, M. Gururajan and L. W. K. Chung, *Cancer Res.*, 2011, **71**, 2600–2610.
- A. Sharma, J. F. Arambula, S. Koo, R. Kumar, H. Singh, J. L. Sessler and J. S. Kim, *Chem. Soc. Rev.*, 2019, **48**, 771–813.
- J. B. Wu, C. Shao, X. Li, Q. Li, P. Hu, C. Shi, Y. Li, Y. T. Chen, F. Yin, C. P. Liao, B. L. Stiles, H. E. Zhou, J. C. Shih and L. W. K. Chung, *J. Clin. Invest.*, 2014, **124**, 2891–2908.
- X. Q. Chen, T. Pradhan, F. Wang, J. S. Kim and J. Yoon, *Chem. Rev.*, 2012, **112**, 1910–1956.
- H. W. Liu, K. Li, X. X. Hu, L. M. Zhu, Q. M. Rong, Y. C. Liu, X. B. Zhang, J. Hasserodt, F. L. Qu and W. H. Tan, *Angew. Chem., Int. Ed.*, 2017, **56**, 11788–11792.
- X. L. Xie, J. L. Fan, M. W. Liang, Y. Li, X. Y. Jiao, X. Wang and B. Tang, *Chem. Commun.*, 2017, **53**, 11941–11944.
- B. Fulton and P. Benfield, *Drugs*, 1996, **52**, 450–474.
- M. Meldal and C. W. Tornøe, *Chem. Rev.*, 2008, **108**, 2952–3015.
- S. A. Kularatne, Z. G. Zhou, J. Yang, C. B. Post and P. S. Low, *Mol. Pharmacol.*, 2009, **6**, 790–800.